Int. Journ. of Lasers in Eng., Vol. 42, pp. 15–29
Reprints available directly from the publisher.
Photocopying permitted by license only.

Characterization of a Yb:YAG Disk Laser Line Welder for Ultra-thin Steel Strip in Industrial Cold-Rolling Mill

J. CHOI*

Advanced Forming Process R&D Group, Korea Institute of Industrial Technology, 44413, Ulsan, Korea

A laser line welder that uses a Yb:YAG disk laser was manufactured and applied to produce ultra-thin coils by continuous operation in a cold-rolling mill. The coils welded range from 0.15 to 0.30 mm in thickness and from 800 to 1100 mm in width. Because the strip is very thin compared to its width, the laser line welding is likely to cause defects such as pinholes on the weld bead. Depending on the diameter of pinholes, the hole-shaped defects on the seam can significantly reduce weld quality including tensile strength and bending strength. To prevent generation of such defects, a hydraulic control device is integrated into the laser line welder so that the positions for cutting and welding the coils by laser are placed within ±30 μm of the target; furthermore, to avoid weld failure, a vision system has been optimized for real-time inspection of the weld zone and detection of weld defects both before and after welding.

Keywords: Yb:YAG disk laser, laser line welder, ultra-thin coil, weld quality inspection, steelworks, cold-rolling mill

1 INTRODUCTION

A welder is one of the most important facilities in the steel industry for continuous operation of cold-rolled steel processes such as continuous annealing line, pickling and cold-rolling mill, re-coiling line, continuous galvanizing

*Corresponding author: E-mail: junchoi@kitech.re.kr

line and manufacturing process of electrical steel, stainless steel and wire [1-3]. If the welder does not operate reliably, the welded strip could break during subsequent operations; such failures cause serious productivity loss, and cost time and manpower for repairs. Thus, to prevent the rupture of welded strip and make the operation reliable, the welds should have higher tensile strength and flexural strength than those of the base metal.

A variety of welders have been developed in accordance with the conditions and characteristics of each production line [4-6]. Depending on the type of heat source energy used for welding, the welding equipment is classified as flash butt welder, seam welder, arc welder, plasma welder and laser welder [7-9]. In particular, the laser welder has actively been developed to meet recent new demands due to the emergence of several alloyed steels [10-13].

Conventionally, a CO_2 laser has been used for various applications in the steelworks [14-16]; however, the dusty environment of making steel and iron causes many problems. The copper mirror for the CO_2 laser beam delivery could be easily contaminated by the dust particles and make the efficiency low [17].

In this work, a Yb:YAG disk laser line welder was developed, as detailed in Table 1, to produce ultra-thin steel coils in the cold-rolling process in a steelworks, and its reliability was characterized. The beam delivery method based on an optical fiber of the disk laser can reduce the cost and manpower requirement for maintenance [18, 19]. The laser line welder was to cut and weld steel strips with a single laser generator in actual industries. The Yb:YAG disk laser line welder integrates a diversity of technology such as a controller,

TABLE 1
Details of the laser line welder used.

Category	Item	Specification
Coil (Strip)	Thickness (mm)	0.15 to 0.30
	Width (mm)	800 to 1100
	Tensile strength (MPa)	501 to 600
	Type of coil	Black plate
Laser	Gain material	Yb:YAG
	Wavelength (nm)	1030
	Maximum output power	4
	Beam delivery	Optical fiber
	Diameter of beam spot (μm)	200
Welder	Cutting method	Laser
	Cutting speed (m/min)	10 to 15
	Welding speed (m/min)	10 to 15
	Shielding gas	N_2

sensors, machinery, hydraulic components and database. Particularly, because the butt-welded steel strip was extremely thin and wide, elimination of gap formation and optical alignment with the laser were critical [20, 21]. Inadequate control of the gap causes severe weld defects [22, 23]. To overcome this problem, a precise hydraulic system and linear variable differential transformer (LVDT) sensors were used to control the position of the two strips welded. In addition, the weld quality monitoring system was optimized to determine in real-time, whether or not the welding status of the coils is good. To verify the weld quality, the gap and weld bead was observed before, during and after welding. This paper introduces characterization of the laser line welder that uses a Yb:YAG disk laser in practical field, and the system integration technology to improve the precision and accuracy of welding and to minimize the occurrence of pinhole flaws.

2 EXPERIMENTAL DETAILS

2.1 Experimental setup and fundamental approaches

A disk laser (TruDisk 4002; TRUMPF, GmbH) that uses Yb:YAG as a gain material was used in this work. The wavelength was 1030 nm and the maximum laser power was 4 kW. The beam quality was 8 mm·rad and the minimum diameter of the laser light cable was 200 μm.

A single laser source was applied for cutting and welding of ultra-thin steel plate and the cutting and welding speed are 10 to 20 m/min. The laser beam was transmitted through optical fibres to weld and cut the steel strip separately. N_2 gas was used to shield the weld zone. The thickness of the coils ranges from 0.15 to 0.30 mm and the width from 800 to 1100 mm. Because the welded coils are extremely thin and wide, the clamp control to determine the positions of welding and cutting the strip must be both accurate and precise. In this work, a precise control system was implemented by using a proportional hydraulic control method. Although the viscosity of the hydraulic oil is affected by the ambient temperature and consequently the precision of control is slightly changed, the welding part reliably avoids rupture of cold-rolled steel sheets in the thickness range 0.15 to 0.30 mm.

The welding zone was observed before, during and after welding. Two CCD cameras and a laser scanner (Q4 20/10; QuellTech, GmbH) were used to inspect the welding in real time. The laser scanner is capable of covering the range of 20 mm in the z-direction and 12 mm in the x-direction. In this case, the z direction is perpendicular to the weld seam and the x direction is horizontal to the weld seam. When the laser scanner operates at a standoff of 53 mm from the weld seam, the measurement resolution is about 13 to 15 μm. Before welding, the geometry of the gap welded was measured by a line-shaped laser sensor; during welding, the shape of the plasma generated by laser welding was monitored; after welding, the weld defects including pin-

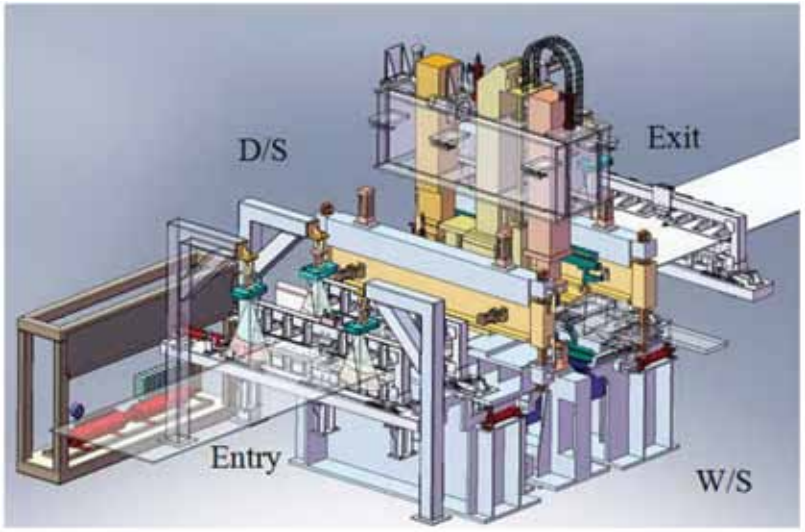

FIGURE 1
Schematic overview of the laser line welder for continuous production in cold-rolling mill (D/S: drive side, W/S: work side).

holes on the bead were detected to assess the welding quality. Finally, a tensile strength test was conducted off line to confirm the weld quality.

2.2 Configuration of laser line welder

The Yb:YAG laser line welder consists of an adjustment unit to align two the coils welded before welding, a clamping unit to determine the position of cutting and welding, a sensor unit to monitor the welding quality and the hydraulic unit to drive machinery (Figure 1). For convenience, the laser line welder is divided into four parts: entry, exit, work side (W/S) and drive side (D/S). The coil to be welded comes in through the entry and goes out through the exit. The welding is performed in one direction from W/S to D/S. In the entry and exit sides, both strips are aligned and fixed by a clamping device and a centering device, repectively.

The upper and lower carriages are located at the centre of the laser line welder. The upper carriage has two cutting heads to shear the entry and exit of strips at the same time and a single welding head to join the strips. Two rolls are positioned slightly ahead of the welding head to remove any mismatch in the gap between the two strips, because such gaps could cause weld defects. After welding, the weld part is planished by other rolls to finalize the welding.

2.3 Cutting and welding methodology

The laser line welder was used for both cutting and welding the strip without the use of a mechanical shear. When the strip is cut, two cutting heads with a

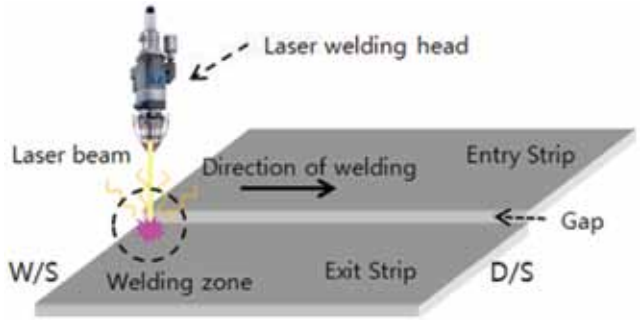

FIGURE 2
Schematic of the welding for two strips with the Yb:YAG laser line welder.

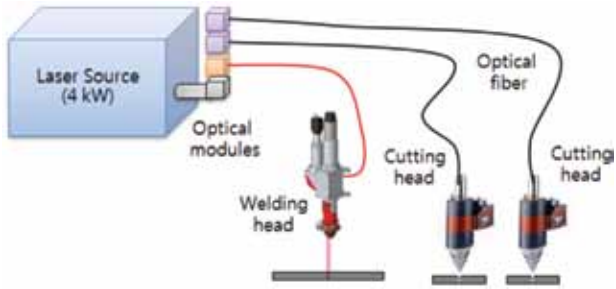

FIGURE 3
Schematic diagram showing the control of the laser beam delivery for cutting and welding with a single laser generator.

single laser source are used to cut both entry and exit strip at the same time. In this process (*cf.* Figure 2), the laser power is equally divided into two cutting heads from a single laser generator (*cf.* Figure 3). Because the laser power required does not exceed 2 kW for cutting with a thickness range of 0.15 to 0.30 mm, it can cut both sides of strips at once with a laser oscillator that has maximum power of 4 kW. After cutting the strip, the two strips are aligned to the welding position, and sequentially welded with a single welding head. The maximum cutting speed was up to 15 m/min considering the thickness of the strip; the welding speed is 10 to 15 m/min. The total cycle time, taking into account cutting and welding speed is <90 seconds.

2.4 Clamping device

To obtain stable welding quality and to avoid breakage of the welded strip during successive processes, the alignment between the gap and the laser must be both accurate and precise [24]. In the particular case of an ultra-thin strip less than 0.5 mm in thickness, the reproducibility of the stop positions of the clamp

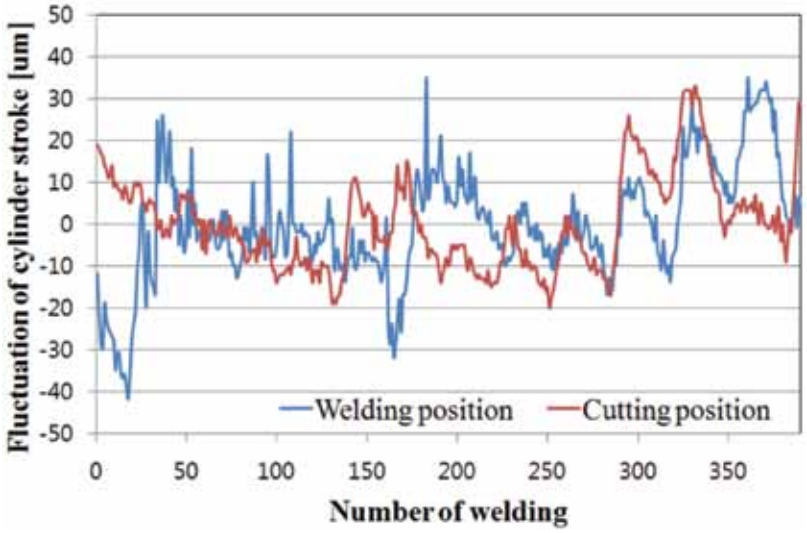

FIGURE 4
Plot of the results of the precision control by the hydraulic system for cutting and welding positions.

to cut and weld the strip is critical. The clamping device moves the strip to the specific position and stops it there. A precise control system enables the clamp to accurately track the cutting and welding positions for laser butt-welding of ultra-thin strips. The clamp is composed of a hydraulic cylinder and valve to drive the clamp, an LVDT sensor to monitor the cylinder stroke, a pair of stoppers and a control algorithm to control the speed of the cylinder. The cylinder strokes of W/S and D/S are monitored and controlled by a programmable logic controller (PLC) according to the operation condition. The stopping positions of the clamp must not change over time. If the positions fluctuate, the change must be promptly corrected to ensure continuous good welding quality. The cutting and welding fluctuated slightly on a diurnal basis, as can be seen in Figure 4; the reason may be that temperature difference between day and night affects the viscosity of the hydraulic fluid, and so results in a slight fluctuation in the cutting and welding positions. The zero value is the reference of the clamp position and most of the errors of control were within ±30 μm.

3 RESULTS AND DISCUSSION

3.1 Gap measurement

When the ends of strips to be welded face each other at the welding position, the gap configuration between the strips has a strong effect on the quality of the laser welding. In the case of ultra-thin strip, 0.15 to 0.30 mm in thickness,

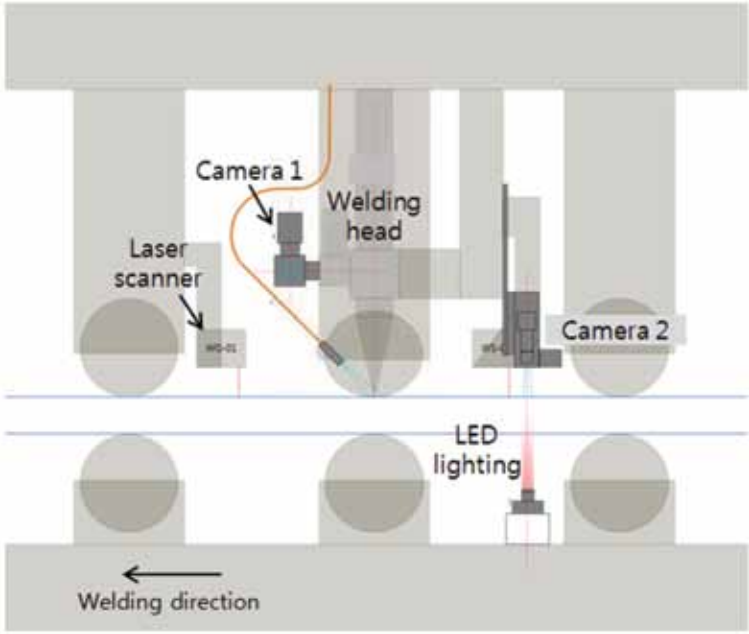

FIGURE 5
Schematic diagram showing the configuration of the vision system of the Yb:YAG laser line welder used to identify and inspect weld defects.

the gap geometry has a great influence on the formation of weld defects during welding. Therefore, the gap between two strips must be monitored when welding. To avoid weld defects, any misalignment or mismatch in the gap should be removed before welding proceeds. In the laser line welder, the weld seam is inspected using a vision system that consists of two CCD cameras and a laser scanner, and is conducted before, during, and after processing, as shown in Figure 5. The laser scanner measures the gap geometry for the preprocessing before welding. Camera 1 is used to capture in real-time the movement of the plasma plume during welding; Camera 2 creates panoramic images of the weld bead after welding.

A laser scanner is installed at the welding head where the strips are welded by the laser. The sensor scans the geometry of the gap that is formed by both entry and exit strips (see Figure 6(a)). The laser scanner moves across the strip (see Figure 6(a), arrow) so that the distance from the strip surface to the sensor is gathered. Then, gap configurations such as mismatch and gap width are identified by post-processing of the measurement data. A mismatch is defined as a difference in average heights of the strips, and the gap width is defined as the spacing between two strips (see Figure 6(b)). The sensor is located 55 mm above the weld bead and a measurement resolution at the

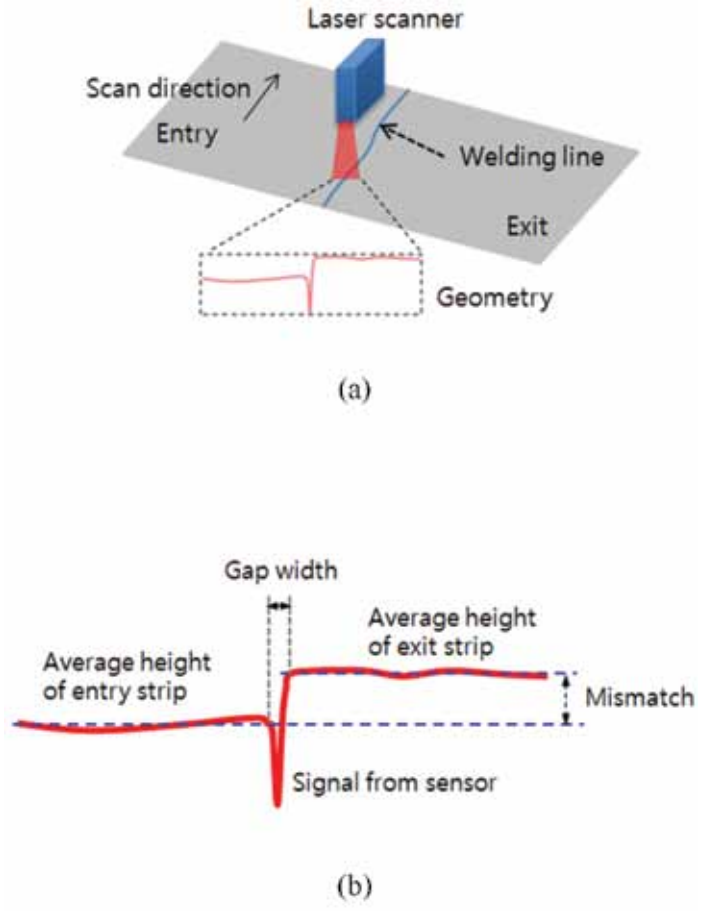

FIGURE 6
Diagrams illustrating (a) the measurement methodology of the gap geometry and (b) magnification of the measured gap geometry.

location is 40 μm in the vertical direction. The scan range of the sensor is approximately 10 to 12 mm across the weld seam and the resolution is 20 μm in the horizontal direction.

The laser scanner installed at the welding head moves along the welding line of the strips and measures the height in the range of 1000 to 1800 mm. Because of this arrangement, the gap can be monitored in real time, as shown in Figure 7(a) and prompt evaluation of the quality of the weld can be made. In this case, the thickness of the strip was 0.17 mm and the mismatch increased toward the middle of the strip. For example, a cross section of the gap at 1500 mm carriage position shown in Figure 7(b) indicates a mismatch >500 μm; the strip is only 0.17 mm thick, so this

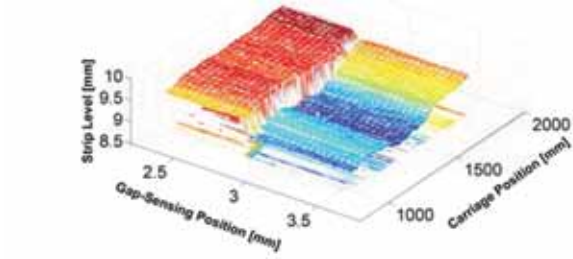

(a)

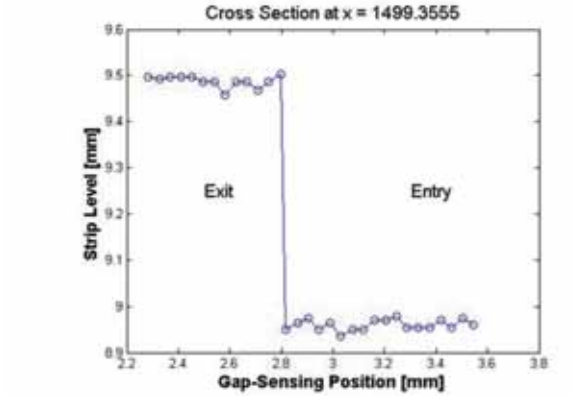

(b)

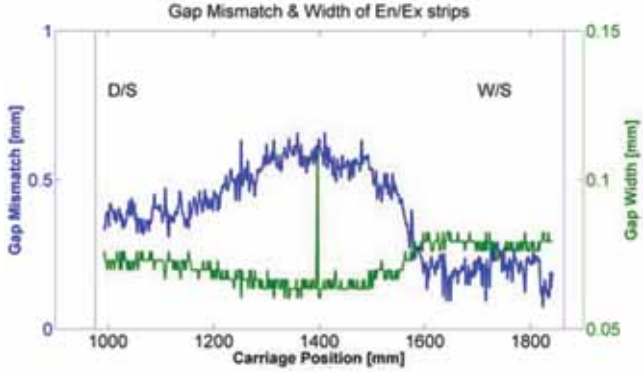

(c)

FIGURE 7
(a) Three-dimensional measurement result of the gap formed by two strips; (b) cross section of the gap at a certain carriage position; and (c) the gap mismatch and width measured from D/S to W/S.

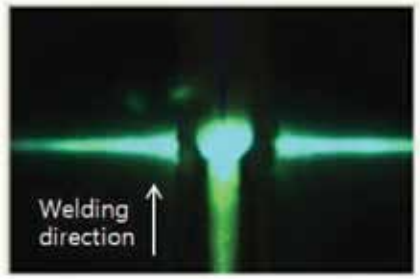

FIGURE 8
Image of the plasma plume generated during the laser line welding of the ultra-thin steel strips.

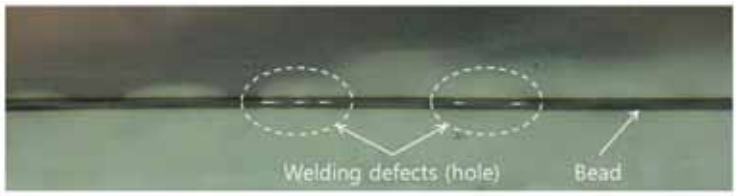

FIGURE 9
Optical micrograph of hole-shaped weld defects in the weld bead of the welded ultra-thin steel strip.

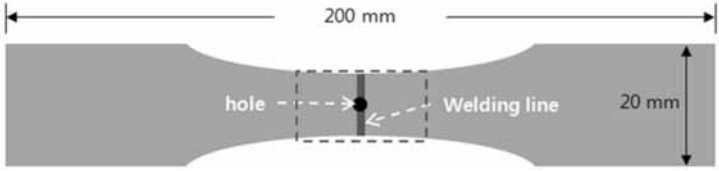

FIGURE 10
Technical drawing of the samples for the tensile strength testing.

mismatch likely to cause weld defects. In this work, two pilot rolls were used to reduce the mismatch right before the laser was beamed at the strip before welding. This use of a pilot roll reduced the mismatch by 10 to 20 μm by pressing both strips, simultaneously. As an example of the overall seen from Figure 7(c), the gap width was <80 μm, but the gap mismatch was >300 μm from D/S to centre of the strip. Because this mismatch is almost twice the thickness, it should be fixed by using the pilot roll to avoid weld defects. In this way, the weld quality can be predicted, and the need for maintenance can assessed based on the information.

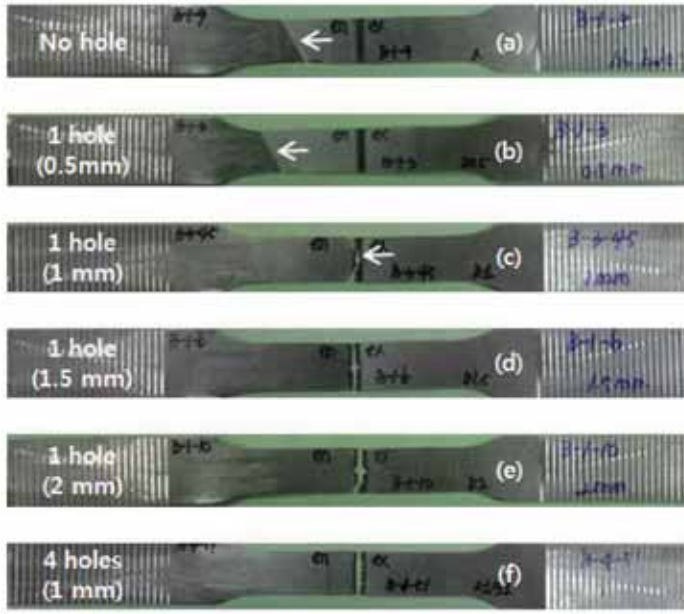

FIGURE 11
Photographs of broken specimens from the tensile tests with (a) no pinhole, (b) 0.5 mm single pinhole, (c) 1.0 mm single pinhole, (d) 1.5 mm single pinhole, (e) 2.0 mm single pinhole and (f) 1.00 mm with four pinholes.

3.2 Welding defects

The laser welding was observed in real time by Camera 1 during welding, as shown in Figure 5. If the gap remains acceptable (no mismatch, gap width <80 μm), the plasma plume is symmetric and has in the direction of welding and a tail in the opposite direction (*cf.* Figure 8), and the laser beam does not leak between the strips. The image in Figure 8 was taken by a 5-Mpixel CCD (Camera 1) equipped with an infrared (IR)-cut filter; the flames on both sides of the plasma plume are reflections of the plume inside the pilot roll.

After welding, the weld bead was observed by Camera 2, as shown in Figure 5. Because the strip welded is ultra-thin, welding defects such as pinholes, except for undercut and porosity may occur on the bead, as is evident from Figure 9. To detect holes, two light emitting diode (LED) sources were used simultaneously: a red LED light to illuminate the underside of the strip; and a white LED to illuminate its upper surface so that Camera 2 can detect holes in the bead. Several samples for tensile strength test were prepared to investigate how the weld quality deteriorates due to hole defects. Each sample was 200 × 20 mm^2 including the welding part generated defects, as shown in Figure 10. In strips that were several hundred micrometers thick, the weld quality could be determined by the size of hole defects generated in the weld zone.

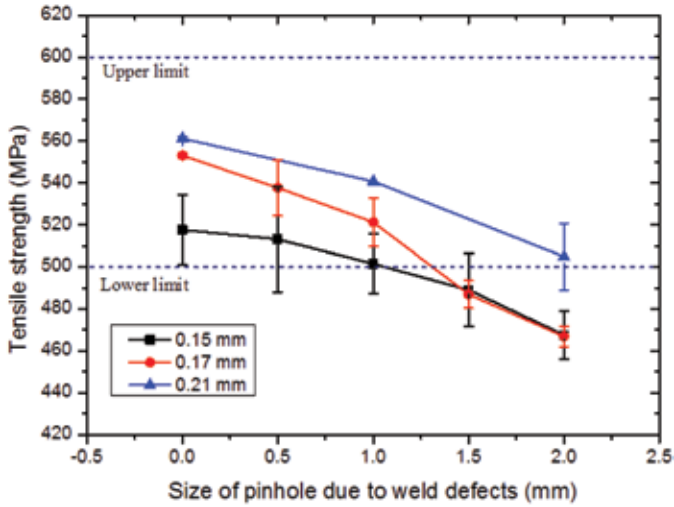

FIGURE 12
Graph showing the tensile strength of the samples with a different diameter of a pinhole defect. Upper and lower limits (501 to 600 MPa) represent the tensile strength of the base metal as a reference.

Tests were conducted and the results are given in Figure 11 to determine how the size and number of weld defect holes affected the strips' tensile strength. This experiment considered two butt-welded strips 0.15 mm thickness. When no weld defects (see Figure 11(a)) or one small hole (0.5 mm diameter) (see Figure 11(b)) were present, the weld quality was not degraded: the base metal broke rather than the welding zone. If the diameter of the hole was >1.0 mm, the weld quality could be degraded, as can be seen from Figures 11(c) to (e); furthermore, the presence of several small holes reduces tensile strength significantly (*cf.* Figure 11(f)) and caused the welding zone to the fracture in the tensile strength test.

The effects of pinhole size changed as strip thickness was increased from 0.15 to 0.21 mm. Measurements given in Figure 12 of tensile strength tests in accordance with the size of the holes were used to determine that maximum tolerable defect size, *Y,* is related to the thickness, *x*, of the strip:

$$Y=2.9\ln(x)+6.6 \quad (1)$$

with an $r^2=0.979$, which indicates a good fit. Pinholes more than 0.5, 1.0 and 1.5 mm in diameter might cause failure of coils of 0.15, 0.17 and 0.21 mm in thickness. Equation (1) can be used to determine the value of Y for other strips with different *x* up to 0.4 mm (Figure 13). The reference based on measurements including Equation (1) and Figure 13 have been applied to the

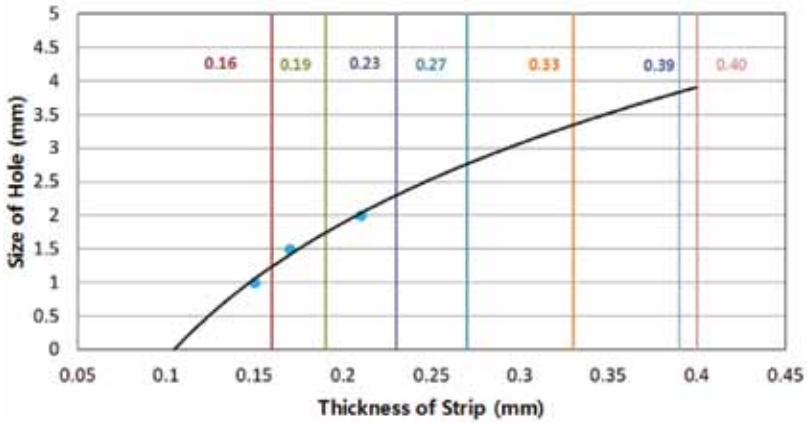

FIGURE 13
Estimation of acceptable diameter of pinhole generated on the weld bead for different thicknesses of strips using a non-linear regression analysis

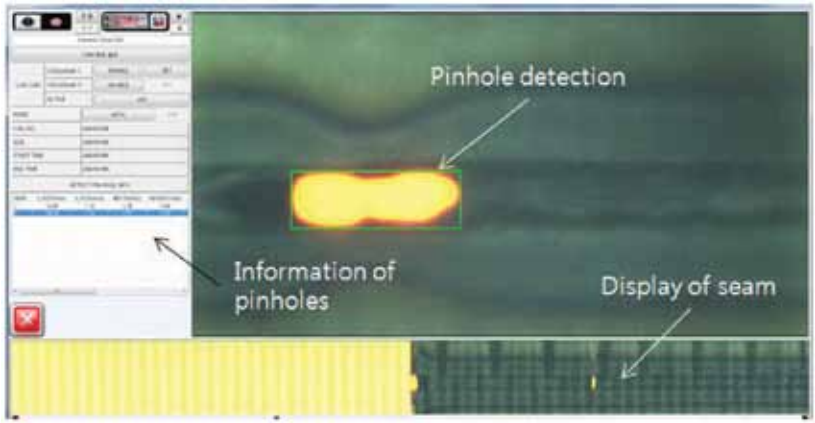

FIGURE 14
Pinhole detection of the weld seam by vision system

Yb:YAG laser line welder monitoring system to determine the weld quality. The information such as size, position and number of the pinholes can be gathered by the vision system (Figure 14).

4 CONCLUSIONS

A laser line welder that uses a Yb:YAG disk laser has been developed and characterized for continuous production of cold-rolled coils. Because the

coils welded are extremely thin, precision control of hydraulic system was integrated into the Yb:YAG laser line welder to guarantee the weld quality. In particular, the clamping device has been optimized using linear variable differential transformer (LVDT) sensors, two stoppers and a PCL control algorithm so that the positions for cutting and welding do not vary among operations. Consequently, the errors for the control of clamp positions were less than ±30 μm, which satisfied the normal operation of the Yb:YAG laser line welder. In addition, the gap geometry of two strips welded was monitored before, during and after processing. Due to the thinness of the strip, most of the weld defects were pinholes on the weld seam. To avoid weld failure, the pinholes of the bead are inspected by a customized vision system and a reference for assessing weld quality was derived on the basis of experimental results. This system will increase the profitability of continuous production of cold-rolled steel strips in the steelworks.

5 ACKNOWLEDGEMENTS

This work was supported by the National Research Foundation of Korea (NRF), grant funded by the Korean Government (MSIP) (No. NRF-2016R1C1B1014508) and conducted with the support of POSCO.

REFERENCES

[1] Hirata T., Kawahara Y., Yairi T., Asano K., Maeda I., Sasaki T. and Machida K. New monitoring technique for detecting buckling in the continuous annealing line using canonical correlation analysis. *SICE Journal of Control, Measurement, and System Integration* **8** (2015), 214-220.

[2] Barjon S., Thomasson H. and Perret J. *Device for the weld joining of sheet metal strips.* US Patent US8445811B2, 21st May 2013.

[3] Sun W.Q., Shao J., Song Y. and Guan J.L. Research and development of automatic control system for high precision cold strip rolling mill. *Advanced Materials Research* **952** (2014), 283-286.

[4] Hariri A., Azreen P.N., Leman A.M. and Yusof M.Z.M. Pulmonary adverse effects of weld bonding process by Malaysia's automobile assembly welders. *Procedia Engineering* **68** (2013), 299-304.

[5] Luo Z., Dai J.S., Wang C., Wang F., Tian Y. and Zhao M. Predictive seam tracking with iteratively learned feedforward compensation for high-precision robotic laser welding. *Journal of Manufacturing Systems* **31** (2012), 2-7.

[6] Eun J.M. and Lee Y.K. A development of overlay GTAW welding system for pipe inside straight process. *Journal of Welding and Joining* **32** (2014), 130-134.

[7] Mahrle A., Schnick M., Rose S., Demuth C., Beyer E. and Füssel U. Process characteristics of fibre-laser-assisted plasma arc welding. *Journal of Physics D: Applied Physics* **44** (2011), 345502.

[8] Liu Y.K., Zhang W.J., Zhang Y.M. A tutorial on learning human welder's behavior: Sensing, modeling, and control. *Journal of Manufacturing Processes* **16** (2014), 123-136.

[9] Ito M., Yokozawa F., Kawai Y. and Tachibana R. Welding characteristics of stainless steel in 10 kW laser beam welder. *ISIJ International* **39** (1999), 737-741.

[10] Lee K.R., Hwang C.Y., Yang Y.S., Park E.K. and Yoo Y.T. The porosity control technology of lap joint welding using continuous wave Nd:YAG laser of the low carbon steel SS41. *Journal of The Korean Society of Manufacturing Technology Engineers* **22** (2013), 665-672.

[11] Yan J., Gao M. and Zeng X. Study on microstructure and mechanical properties of 304 stainless steel joints by TIG, laser and laser-TIG hybrid welding. *Optics and Lasers in Engineering* **48** (2010), 512-517.

[12] Nagel F., Simon F., Kümmel B., Bergmann J.P. and Hildebrand J. Optimization Strategies for Laser Welding High Alloy Steel Sheets. *Physics Procedia* **56** (2014), 1242-1251.

[13] Zhang J., Xu S. and Li Z. Investigation into plastic damage behavior of the CO_2 laser deep penetration welded joint for Ti–6Al–4V alloy. *Engineering Fracture Mechanics* **83** (2012), 1-7.

[14] Anawa E.M. and Olabi A.G. Optimization of tensile strength of ferritic/austenitic laser-welded components. *Optics and Lasers in Engineering* **46** (2008), 571-577.

[15] Mei L., Yan D., Chen G., Xie D., Zhang M., Ge X. Comparative study on CO_2 laser overlap welding and resistance spot welding for automotive body in white. *Materials & Design* **78** (2015), 107-117.

[16] Wu Y., Cai Y., Sun D., Zhu J. and Wu Y. Characteristics of plasma plume and effect mechanism of lateral restraint during high power CO_2 laser welding process. *Optics and Laser Technology* **64** (2014), 72-81.

[17] Papernov S. and Schmid A.W. Laser-induced surface damage of optical materials: absorption sources, initiation, growth, and mitigation. *XL Annual Symposium on Optical Materials for High Power Lasers.* 30 December 2008, Boulder, CO., USA. **7132**, 71321J.

[18] Iqbal S., Gualini M.M.S. and Grassi F. Laser welding of zinc-coated steel with tandem beams: Analysis and comparison. *Journal of Materials Processing Technology* **184** (2007), 12-18.

[19] TRUMPF Technical Documentation Department. *Laser Machining Solid-state Lasers*, TRUMPF GmbH. 2007.

[20] Unt A., Lappalainen E. and Salminen A. Autogenous laser and hybrid laser arc welding of T-joint low alloy steel with fiber laser systems. *Physics Procedia* **41** (2013), 140-143.

[21] Karlsson J. and Kaplan A.F.H. Analysis of a fibre laser welding case study, utilising a matrix flow chart. *Applied Surface Science* **257** (2011), 4113-4122.

[22] Gao X., Zhen R., Xiao Z. and Katayama S. Modeling for detecting micro-gap weld based on magneto-optical imaging. *Journal of Manufacturing Systems* **37** (2015), 193-200.

[23] Mei L., Chen G., Yan D., Xie D., Ge X. and Zhang M. Impact of inter-sheet gaps on laser overlap welding performance for galvanised steel. *Journal of Materials Processing Technology* **226** (2015), 157-168.

[24] Sharma R.S. and Molian P. Weldability of advanced high strength steels using an Yb:YAG disk laser. *Journal of Materials Processing Technology* **211** (2011), 1888-1897.